Atmos. Chem. Phys. Discuss., https://doi.org/10.5194/acp-2019-75
Manuscript under review for journal Atmos. Chem. Phys.
Discussion started: 25 April 2019

Atmospheric Chemistry and Physics Discussions

Molecular characteristics and diurnal variations of organic aerosols at a rural site in the North China Plain with implications for the influence of regional biomass burning

Jianjun Li[1,4], Gehui Wang[1,2,3 *], Qi Zhang[4*], Jin Li[1], Can Wu[2], Wenqing Jiang[4], Tong Zhu[5], and Limin Zeng[5]

[1] Key Lab of Aerosol Chemistry & Physics, SKLLQG, Institute of Earth Environment, Chinese Academy of Sciences, Xi'an 710061, China
[2]Key Laboratory of Geographic Information Science of the Ministry of Education, School of Geographic Sciences, East China Normal University, Shanghai 200241, China
[3]Institute of Eco-Chongming, 3663 N. Zhongshan Rd., Shanghai 200062, China
[4]Department of Environmental Toxicology, University of California, Davis, CA 95616, USA
[5]BIC-ESAT and SKL-ESPC, College of Environmental Sciences and Engineering, Peking University, Beijing, China

*Corresponding authors:
Prof. Gehui Wang, E-mail: ghwang@geo.ecnu.edu.cn;
Prof. Qi Zhang, E-mail: dkwzhang@ucdavis.edu

Atmos. Chem. Phys. Discuss., https://doi.org/10.5194/acp-2019-75
Manuscript under review for journal Atmos. Chem. Phys.
Discussion started: 25 April 2019

Atmospheric Chemistry and Physics Discussions

Abstract

Field burning of crop residue in early summer releases into the atmosphere a large amount of pollutants with significant impacts on the air quality and aerosol properties in the North China Plain (NCP). In order to investigate the influence of this regional anthropogenic activity on organic molecular characteristics of aerosol, we collected $PM_{2.5}$ filter samples every 3 hours at a rural site of NCP during June 10th to 25th, 2013, and analyzed them for more than 100 organic tracer compounds, including both primary (*n*-alkanes, fatty acids/alcohols, sugar compounds, polycyclic aromatic hydrocarbons, hopanes, and phthalate esters) and secondary (phthalic acids, isoprene-, α-/β-pinene, β-caryophyllene, and toluene-derived products) organic aerosol tracers, as well as for organic carbon (OC), elemental carbon (EC), and water-soluble organic carbon (WSOC). Total concentrations of the measured organics ranged from 177 to 6248 ng m^{-3} (mean 1806±1308 ng m^{-3}) during the study period, most of which were contributed by sugar compounds, followed by fatty acids and fatty alcohols. Levoglucosan (240±288 ng m^{-3}) was the most abundant single compound and strongly correlated with OC and WSOC, suggesting that biomass burning (BB) is an important source of summertime organic aerosols in this rural region. Based on analysis of fire spots and backward trajectories of air masses, two representative periods were classified, which are (1) Period 1 (P1), Jun 13th 21:00-16th 15:00, when air masses were uniformly from the southeast part of NCP, where intensified open-field burning of biomass fuels occurred and (2) Period 2 (P2), Jun 22nd 12:00-24th 06:00, which were representative of local emission. Nearly all the

measured PM components showed much higher concentrations in P1 than in P2. Although *n*-alkanes, fatty acids, and fatty alcohols presented similar temporal/diurnal variations as those of levoglucosan throughout the entire period, their molecular distributions were more dominated by high molecular weight (HMW) compounds in P1, demonstrating an enhanced contribution from BB emissions. In contrast, intensified BB emission in P1 seems to have limited influences on the concentrations of polycyclic aromatic hydrocarbons (PAHs), hopanes and phthalate esters. Both 3-hydroxyglutaric acid and β-caryophyllinic acid showed strong linearly correlations with levoglucosan (R^2=0.72 and 0.80, respectively), indicating that biomass burning is also an important source for terpene-derived SOA formation. A tracer-based method was used to access the distribution of biomass-burning OC, fungal-spore OC and secondary organic carbon (SOC) derived from isoprene, α-/β-pinene, β-caryophyllene, and toluene in the different periods. The results showed that the contribution of biomass-burning OC to total OC in P1 (27.6%) was 1.7 times of that in P2 (17.1%). However, the contribution of SOC from oxidation of the four kinds of VOCs increased slightly from 16.3% in P1 to 21.1% in P2.

Key words: Organic aerosols; Molecular composition; North China Plain; Biomass Burning

Atmos. Chem. Phys. Discuss., https://doi.org/10.5194/acp-2019-75
Manuscript under review for journal Atmos. Chem. Phys.
Discussion started: 25 April 2019

Atmospheric Chemistry and Physics Discussions

1. Introduction

Organic aerosols (OA, i.e., the organic fraction of particles) constitute a substantial fraction (~10-90%) (Jimenez et al., 2009;Zhang et al., 2007;Hallquist et al., 2009) of atmospheric particles, and have significant effects on global and regional climate (Venkataraman et al., 2005;Kanakidou et al., 2005), air quality (Aggarwal et al., 2013;Wang et al., 2006b), human health (Lelieveld et al., 2015), and ecosystems (Tie et al., 2016). Organic aerosols in the atmosphere can be emitted directly from various sources, such as combustion of fossil fuels, biomass burning, plant emission, and so on, which is defined as primary organic aerosols (POA). On the other hand, atmospheric secondary OA (SOA) are produced from photochemical oxidation products of volatile organic compounds (VOCs) via gas-particle conversion processes such as nucleation, condensation and heterogeneous chemical reactions (Hallquist et al., 2009). These organic species could modify physicochemical characteristics of atmospheric aerosols such as hygroscopicity, albedo, and oxidation state (Dinar et al., 2008;Chan et al., 2005;Fu et al., 2010). Thus, a thorough understanding of molecular composition and sources of organic aerosols is necessary in order to address aerosol related environmental issues and to improve the accuracy of modelling studies.

Tremendous amounts of air pollutants including both particulate matters (PM) and their gaseous precursors (e.g., SO_2, NO_x, NH_3, and VOCs) are emitted into the atmosphere from power plants, industries and vehicles due to rapid economy development in China, leading to serious air conditions in the recent decades (Zhang et al., 2009;Guo et al., 2014;Wang et al., 2016;Huang et al., 2014;Li et al., 2017). The

North China Plain (NCP) has been recognized as one of the most polluted regions in the world, with very high concentrations of $PM_{2.5}$ on the ground surface (van Donkelaar et al., 2010). The NCP is also considered as one of the most significant aerosol sources, which has a significant impact on the East China Sea and western North Pacific (Andreae and Rosenfeld, 2008). Thus, extensive efforts have been made in recent years to characterize the sources, properties, and processes of PM in the NCP. Most of these results concluded that the severe air pollution in the region is related to the source strength and frequently happens under stagnant weather conditions. Recently, it has been shown that the exponential growth of secondary aerosols could lead to an extreme haze event under certain meteorological conditions (Wang et al., 2016;Sun et al., 2014;Quan et al., 2013).

In the rural area of NCP, biomass burning for domestic cooking and heating and agricultural waste disposal is an important source of atmospheric PM (Wang et al., 2009b;Li et al., 2010;Zhang et al., 2016). Particularly, the open field burning is still a common way for disposal of agricultural residues (mainly wheat straws) in early summer (Li et al., 2007). This traditional activity could release huge amount of pollutants into the atmosphere and significantly affect air quality and aerosol properties in the region. Zhu et al. (2016) examined the amounts of VOCs in the air at a rural site of Yucheng (Shandong Province, East China), and found that their concentrations during the wheat straw burning period are approximately twice of those in normal periods. Model results also revealed a significant influence of open crop residual burning on ozone, CO, black carbon (BC) and organic carbon (OC)

concentrations in NCP. Moreover, both off-line (Fu et al., 2012) and on-line (Sun et al., 2016) observations indicated that the intensified emission from wheat straw burning in the region could change the molecular distribution of organic aerosols of the downwind urban or mountain areas.

During June 10th to 25th of 2013, we conducted a continuous sampling campaign at a rural site in the northern part of NCP. $PM_{2.5}$ filter samples were continuously collected with a 3-hour time resolution and determined for more than 100 organic compounds including aliphatic lipids, sugar compounds, hopanes, polycyclic aromatic hydrocarbons (PAHs), phthalate esters, and secondary oxidation products. The first objective of this study is to get an overall understanding of temporal/diurnal variation and molecular distribution of summertime OA in the rural region. The second objective is to compare the results in two representative periods to investigate the influence of regional field burning of wheat straw on the molecular characteristics of organic aerosols.

2. Experimental section

2.1 Sample collection

The measurement was performed at the Integrated Ecological-Meteorological Observation and Experiment Station of Chinese Academy of Meteorological Sciences (39°08' N, 115°40' E, 15.2 m asl), which is located in a rural area of Gucheng, Hebei Province. Detailed information of the station and sampling campaign was described in Li et al. (2018). Briefly, $PM_{2.5}$ samples were collected on the rooftop (about 10 m above the ground) of a three-story building on the campus of the Gucheng station.

Atmos. Chem. Phys. Discuss., https://doi.org/10.5194/acp-2019-75
Manuscript under review for journal Atmos. Chem. Phys.
Discussion started: 25 April 2019

The sampling was conducted from June 10th to 25th, 2013 by using a high volume (1.13 m^3 min^{-1}) sampler (Anderson) with a three hour of duration in each. All samples were collected onto pre-baked (450 ºC, 6-8 hr) quartz fiber filters. Field blank samples were also collected by mounting blank filters onto the sampler for about 15 min without pumping any air. After sampling, the sample filter was individually sealed in aluminum foil bags and stored in a freezer (−20 ºC) prior to analysis.

2.2 Organic compounds determination

A size of 12.5-25 cm^2 of the filter sample was cut and extracted with a mixture of dichloromethane and methanol (2:1, v/v) under ultrasonication. The extracts were concentrated using a rotary evaporator under vacuum conditions and then blow down to dryness using pure nitrogen. After reaction with N,O-bis-(trimethylsilyl) trifluoroacetamide (BSTFA) at 70 ℃ for 3 hrs., the derivatives were determined using gas chromatography/electron ionization mass spectrometry (GC/EI-MS) (Li et al., 2013b).

Gas chromatograph/mass spectrometry (GC/MS) analysis of the derivatized fraction was performed using an Agilent 7890A GC coupled with an Agilent 5975C MSD. The GC separation was carried out on a DB-5MS fused silica capillary column with the GC oven temperature programmed from 50℃ (2 min) to 120℃ at 15℃ min^{-1} and then to 300℃ at 5℃ min^{-1} with a final isothermal hold at 300℃ for 16 min. The sample was injected in a splitless mode at an injector temperature of 280℃, and scanned from 50 to 650 Daltons using electron impact (EI) mode at 70 eV.

GC/MS response factors of all the target compounds were determined using

authentic standards except several isoprene-derived SOA tracers. Response factors of isoprene-derived SOA tracers were substituted by those of related surrogated standards, which were described in Li et al. (2018). No significant contamination (<5% of those in the samples) was found in the blanks. Recoveries of all the target compounds ranged from 80% to 120%. Data presented were corrected for the field blanks but not corrected for the recoveries.

2.3 OC, EC, and WSOC analysis

OC (organic carbon) and EC (elemental carbon) were analyzed using DRI Model 2001 Carbon Analyzer following the Interagency Monitoring of Protected Visual Environments (IMPROVE) thermal/optical reflectance (TOR) protocol. A size of 0.526 cm^2 sample filter was placed in a quartz boat inside the analyzer and stepwise heated to temperatures of 140 ℃ (OC1), 280 ℃ (OC2), 480 ℃ (OC3), and 580 ℃ (OC4) in a non-oxidizing helium (He) atmosphere, and 580 ℃ (EC1), 740 ℃ (EC2), and 840 ℃ (EC3) in an oxidizing atmosphere of 2% oxygen in helium. Pyrolyzed carbon (PC) is determined by reflectance and transmittance of 633 nm light. One sample was randomly selected from every 10 samples and re-analyzed. Differences determined from the replicate analyses were <5% for TC, and <10% for OC and EC.

Another aliquot of filter sample was extracted with organic-free Milli-Q water under ultrasonication (15 min each, repeated 3 times) and filtered through a PTFE filter to remove any particles and filter debris. Then the water-extract was analyzed for water-soluble organic carbon (WSOC) using a TOC analyzer (TOC-L CPH,

Shimadzu, Japan). The difference between OC and WSOC was considered as water-insoluble OC (WIOC). All carbonaceous components data reported here were corrected by the field blanks.

3. Results and discussion

3.1 Fire spots and air masses

At present, open-field burning is still a common activity for disposal of crop residue in the rural area of the North China Plain, especially during wheat harvest period from the end of May to the middle of June (Fu et al., 2012). These extensive emissions from regional biomass burning in the provinces of Anhui, Jiangsu, Shandong, Henan and Hebei in the NCP can cause severe air pollution on a local and regional scale. In our previous study, the fire spots in the North China during the sampling period were provided based on the NASA satellite observation (https://firms.modaps.eosdis.nasa.gov/firemap/). Combining with information on air mass back-trajectories (http://ready.arl.noaa.gov/HYSPLIT.php), the sampling period was divided into two sections: (1) June 10-18, when air masses were mainly transported via long distances from the southeast part of NCP where intensive emissions from the wheat straw burning occurred; (2) June 19-25, when air masses were mostly influenced by local emissions and regional emission from biomass burning decreased dramatically (Li et al., 2018). In this study, we further select two representative periods to access the contribution of regional biomass burning. Period 1 (P1) designates 13th Jun 21:00 pm to 16th Jun 15:00 pm, during which air masses were influenced by intensive biomass burning and transported uniformly from the southeast

Atmos. Chem. Phys. Discuss., https://doi.org/10.5194/acp-2019-75
Manuscript under review for journal Atmos. Chem. Phys.
Discussion started: 25 April 2019

Atmospheric Chemistry and Physics Discussions

part of NCP (Figure 1 a and b, and Figure S1). Period 2 (P2) designates 22nd Jun 12:00 pm to 24th Jun 06:00 am, during which fire spots in the regions were relatively scarce and air masses came predominantly from the surrounding areas of the sampling site (Figure 1 c and d). In addition, there were several intermittent rainfalls during June 20-22, which are favorable for wet deposition of atmospheric pollutants. Thus, aerosols collected in P2 are well representative of local fresh emission. It is worthwhile to note that the two samples collected during 21st June 18:00-24:00 pm were excluded from P2, because they were highly affected by near-site biomass burning emission (detailed information is provided in Section 3.3).

3.2 Concentrations of $PM_{2.5}$, OC, EC, WSOC and WIOC

Concentrations of $PM_{2.5}$ and carbonaceous components are presented in Table 1. $PM_{2.5}$ concentrations range from 21 to 395 μg m^{-3} with a mean value at 159±89 μg m^{-3} during the whole sampling period. As shown in Figure 2, $PM_{2.5}$ concentrations in P1 (average ± 1σ = 231±89 μg m^{-3}) increase continuously from around 150 μg m^{-3} to higher than 300 μg m^{-3}, indicating the occurrence of a severe air pollution episode. In contrast, $PM_{2.5}$ concentration during P2 is as low as 43±14 μg m^{-3}. Similarly, the average concentration of OC is 29.4±7.8 μg m^{-3} in P1, which is more than 5 time higher than that in P2 (5.5±1.7 μg m^{-3}) . EC concentrations also decrease dramatically from P1 (12.1±4.0 μg m^{-3}) to P2 (1.5±1.5 μg m^{-3}). The average OC/EC ratio is 3.0±0.9 for the whole sampling period, but the ratio was higher in P2 (3.8±1.0) than in P1 (2.5±0.4), mainly due to the high SOA formation activities in the rural areas of NCP in summer.

Atmos. Chem. Phys. Discuss., https://doi.org/10.5194/acp-2019-75
Manuscript under review for journal Atmos. Chem. Phys.
Discussion started: 25 April 2019

Atmospheric Chemistry and Physics Discussions

As shown in Figure 2 and 3, the concentrations of WSOC show a consistent temporal variation as those of OC (R^2=0.82), highlighting the fact that WSOC is an important fraction of OC in this region. In addition, the average ratio of WSOC/OC is higher during P1 (0.62±0.16) than during P2 (0.48±0.12), mainly due to enhanced emissions of water-soluble organic compounds (such as sugars, fatty alcohols/acids) from biomass burning during P1. Due to the favorable meteorological conditions, concentrations of water-insoluble OC in P2 (3.0±1.3 μg m^{-3}) are also much lower than those in P1 (10.3±4.4 μg m^{-3}).

The diurnal variation profiles of EC/OC and WSOC/OC are shown in Figure 4. EC/OC is generally lower in daytime and the lowest value occurred during 12:00-15:00 pm, mainly due to enhanced daytime formation of SOC. Previous studies have shown that secondary organic aerosols are mainly composed of water-soluble compounds, e.g., polyacids/polyalcohols and phenols (Kondo et al., 2007;Wang et al., 2009a). However, these compounds can come from primary emissions as well, especially from biomass burning (Shen et al., 2017;Fu et al., 2012). In this study, the WSOC/OC presents lower value during daytime, especially in the afternoon when photo-chemical oxidation is favorable. In addition, the diurnal variation pattern of WSOC/OC is similar to that of levoglucosan/OC. Given that levoglucosan is a well-known marker of biomass burning emissions (Simoneit et al., 1999;Simoneit et al., 2004a) (detailed discussions are given in Section 3.3), these results indicate that particulate WSOC in the region is mostly contributed by direct emissions from biomass burning in the summer.

3.3 Organic molecular composition

More than 100 organic species were detected in the aerosol samples, and their concentrations are shown in Table 2 and S1. In this study, these organic compositions are grouped into 10 compound classes based on functional groups and sources. Total concentrations of the measured organics range from 177 to 6248 ng m^{-3} (average = 1806±1308 ng m^{-3}) during the whole sampling period with the predominance of sugar compounds, followed by fatty acids and fatty alcohols. The temporal variation profiles of the determined organic groups are shown in Figure 5. Nearly all the measured organic species, especially *n*-alkanes, fatty acids, fatty alcohols, sugar compounds, and PAHs, show much higher concentrations in P1 than in P2 (Figure S2), indicating an important influence of regional biomass burning on airborne organic aerosols in NCP.

3.3.1 Biomass-burning tracers

As described in Section 3.1, intensified emissions of open biomass burning were observed in the southern part of NCP during June 13-16 (P1), which is an important reason for the severe regional air pollution during this period. Levoglucosan, which is produced in large quantities during pyrolysis of cellulose, is a key tracer for biomass burning emissions (Simoneit, 2002;Simoneit et al., 1999). As shown in Table 2, levoglucosan is the most abundant single compound in the whole sampling period, ranged from 5.6 to 1447 ng m^{-3} with a mean concentration of 240±288 ng m^{-3}. Levoglucosan shows good positive correlations with both OC (R^2=0.61) and WSOC (R^2=0.65) (Figure 3), confirming that biomass burning is an important source of both

aerosol OC and WSOC in the rural region of NCP during the sampling period. As clearly shown in Figure 6, the concentrations of levoglucosan present a continual increasing trend during P1 with a mean value of 404±344 ng m^{-3}. However, the tracer presents very low concentrations (11-123 ng m^{-3}) for the most of time during Jun 20-22. Interestingly, the concentration of levoglucosan suddenly increased by more than 10 times at 21st Jun 18:00 pm to approximately 1200 ng m^{-3} in less than 3 hours and decreased to its beginning concentration (less than 100 ng m^{-3}) within 6 hours (2 samples) afterwards. The concentrations of OC, WSOC and EC also showed obvious peaks during this event. However, based on analyses of back-trajectories (Figure 1c) and wind conditions (Figure S1), we didn't find significant change of air masses origins. Also, not all organic markers showed similar variation as levoglucosan, especially the concentrations of PAHs, hopanes, and phthalate esters changed little during this event. Thus, it is plausible to conclude that this variation was caused by emissions from biomass burning activities nearby the sampling site. For this reason, the data of the 2 samples were excluded from P2.

The two isomers of levoglucosan, galactosan and mannosan, are also produced by the pyrolysis of cellulose/hemicelluloses (Simoneit, 2002), and thus also considered as important markers of biomass burning. Similar to levoglucosan, the concentrations of these two anhydrosugars in P1 are 5-6 times higher than those in P2. The isomeric ratios of levoglucosan to other anhydrosugars are considered as good indicators of straw burning. For example, mannosan and galactosan were detected at low levels in the smoke of lignites (Fabbri et al., 2009;Fabbri et al., 2008). As shown

in Table 2, the ratios of levoglucan/mannosan (L/M) and levoglucan/(galactosan+mannosan) (L/G+M) both showed higher values in P1 than in P2, agreeing well with the results reported by Fu et al. (2012) at Mt. Tai. These results confirmed the great contribution of open burning of wheat straw to the organic aerosols in the sampling region during P1.

3.3.2 Aliphatic lipid compositions

The average concentrations of all the *n*-alkanes (C_{18}–C_{36}) measured in this study is 207±149 ng m^{-3} with the most abundant individual compound being nonacosane ($C_{29}H_{60}$), i.e., the carbon number maximum (C_{max}) is C_{29} (Table S1). *n*-Alkanes derived from terrestrial plants are dominated by high molecular weight species (HMW, carbon number >25) with an odd number preference. In contrast, fossil fuel derived *n*-alkanes do not have odd/even number preference (Rogge et al., 1993b;Simoneit et al., 2004b). In general, *n*-alkanes with a carbon preference index (CPI, odd/even) more than 5 are considered as plant wax, while those with a CPI nearly unity are mostly derived from fossil fuel combustion (Rogge et al., 1993b, a). In this study, the mean value of CPI is 2.47±1.12, indicating that both fossil fuel and plant wax contributed to *n*-alkanes in the rural areas of NCP in summer. However, *n*-alkanes showed a stronger odd/even carbon number predominance in P1 (CPI=2.85) than in P2 (CPI=1.64). In addition, all the low molecular weight *n*-alkanes (LMW, carbon number <25) presented a higher contribution to total *n*-alkanes in P2 than in P1 (Figure 7 a and d). These results demonstrate that plant waxes from biomass burning emissions made a bigger contribution to organic aerosols in the sampling region

Atmos. Chem. Phys. Discuss., https://doi.org/10.5194/acp-2019-75
Manuscript under review for journal Atmos. Chem. Phys.
Discussion started: 25 April 2019

Atmospheric Chemistry and Physics Discussions

during P1.

A homologous series of 19 saturated fatty acids ($C_{12:0}$–$C_{32:0}$) and 3 unsaturated fatty acids ($C_{16:1}$, $C_{18:1}$, and $C_{18:2}$) were detected in the samples (Table S1), and their total concentrations were 514±384 ng m^{-3} during the whole period. A strong even carbon number predominance was observed with C_{max} at $C_{28:0}$ and $C_{16:0}$ (Table S1). Higher molecular weight (HMW) fatty acids ($\geqslant C_{20}$) are derived from terrestrial plant waxes, while LMW fatty acids ($\leqslant C_{19}$) have multiple sources such as vascular plants, microbes and marine phytoplankton as well as kitchen emissions (Rogge et al., 1993a;Kawamura et al., 2003). The total concentrations of fatty acids presented similar temporal variation to levoglucosan and well linearly correlated with it (R^2=0.72) (Figure 8a), indicating that fatty acids are mostly affected by biomass burning emission during the whole sampling period. Still, there are some evidences that regional emission from wheat straw burning significantly affected the distribution of fatty acids in the aerosols of Gucheng during P1. Firstly, the total concentrations of fatty acids in P1 (900±358 ng m^{-3}) are more than 6 times higher than those in P2 (145±48 ng m^{-3}). Secondly, the concentrations and relative contributions of HMW fatty acids ($C_{20:0}$–$C_{32:0}$) are much higher in P1 than in P2, similar to the results of *n*-alkanes. In addition, the mean value of CPI of HMW fatty acids in P1 (4.21±1.14) is also higher than that in P2 (3.50±1.64).

Fatty alcohols in the range of C_{22}–C_{30} were detected for the $PM_{2.5}$ samples with a mean concentration of 193±187 ng m^{-3} (Table 2 and S1) during the whole sampling period. Their distributions are characterized by even carbon number predominance

Atmos. Chem. Phys. Discuss., https://doi.org/10.5194/acp-2019-75
Manuscript under review for journal Atmos. Chem. Phys.
Discussion started: 25 April 2019

Atmospheric Chemistry and Physics Discussions

with a maximum at C_{28} (Figure 7c and f). HMW fatty alcohols ($\geqslant C_{20}$) abundantly present in higher plants and loess deposits (Wang and Kawamura, 2005), thus the total concentration of fatty alcohols strongly correlated with levoglucosan (R^2=0.73) (Figure 8b). Similarly, nearly 10 times higher concentration of fatty alcohols was observed in P1 (322±151 ng m^{-3}) compared with those in P2 (34±23 ng m^{-3}).

3.3.3 Primary saccharides

In addition to the three anhydrosugars, 4 primary sugars (fructose, glucose, sucrose and trehalose) and 3 sugar alcohols (arabitol, mannitol and inositol) were detected in the samples. Primary saccharides have been used as biomarkers for primary biota emissions (Wang et al., 2011). Their mean concentrations ranged from 3.6 to 49 ng m^{-3} during the whole sampling period. In this study, concentrations of fructose, sucrose and trehalose in P1 were 7-10 times higher than those in P2 (Table S1). They well correlated with levoglucosan (R^2=0.47-0.62, Figure S3) during P1, in contrast to P2, during which no relationships were found between them. These results indicated that these primary sugars were also affected by open-field emissions of biomass burning during P1. Sugar alcohols, mainly arabitol and mannitol, are abundant in airborne fungal spores (Graham et al., 2002). Some studies suggested that biomass burning activities can enhance the emission of sugar alcohols at a certain level (Engling et al., 2009;Fu et al., 2012). However, no significant relationship (R^2<0.10) can be found between these sugar alcohols and levoglucosan even in P1, indicating the negligible contribution of biomass burning to the tracers in this study.

3.3.4 PAHs, Hopanes and Phthalates

Atmos. Chem. Phys. Discuss., https://doi.org/10.5194/acp-2019-75
Manuscript under review for journal Atmos. Chem. Phys.
Discussion started: 25 April 2019

As shown in Figure 5, the temporal variation of PAHs, hopanes, and phthalate esters were clearly different to those of the molecular tracers for biomass burning, especially in P1. In contrast to the continuous increase of sugars, fatty acids, fatty alcohols, and n-alkanes during P1, the concentration of PAHs, hopanes, and phthalate esters showed obvious day-night variations, indicating that biomass burning activities contributed little on these species. Phthalates are widely used as plasticizers in synthetic polymers or softeners in polyvinylchlorides (PVC) (Simoneit et al., 2004b) and can be directly emitted from the matrix into the air as they are not chemically bonded with the matrix. Six phthalate esters were detected in the sampling aerosols, i.e., dimethyl (DMP), diethyl (DEP), diisobutyl (DiBP), butyl isobutyl (BiBP), di-n-butyl (DnBP), and bis(2-ethylhexyl) (BEHP) phthalates (Table S1). The concentrations of total detected phthalate esters in P1 (112±33 ng m^{-3}) are around 2 times only higher than those in P2 (51±18 ng m^{-3}). Hopanes are abundant in coal and crude oils and enriched in lubricant oil fraction (Oros and Simoneit, 2000;Kawamura et al., 1995).They can be emitted to the atmosphere from coal burning and/or internal combustion of fuel in engines. Only two dominant hopanes, 17α(H),21β(H)-30-norhopane($C_{29\alpha\beta}$) and 17α(H),21β(H)-hopane($C_{30\alpha\beta}$), were detected in all of the samples in this study. Their average concentration in P1 (4.40±2.48 ng m^{-3}) is ~ 2.5 times of that in P2 (1.81±0.31 ng m^{-3}). Considering the much higher concentrations of levoglucosan in P1 (on average ~ 8 times higher than P2), these results again confirmed a limited influence of biomass burning on concentrations of phthalate esters and hopanes in the aerosols in the rural region. Thus, there were no

significant concentration changes of the two species at 21st Jun 18:00-24:00 pm, when the air masses were highly affected by nearby biomass burning activities.

PAHs are the products of incomplete combustion of carbon-containing materials and are of high toxicity and carcinogenicity (Halek et al., 2008;Sultan et al., 2001). Previous studies indicated that PAHs are mainly emitted from coal burning and vehicle exhaust in most areas of China (Wang et al., 2006a). However, it has been reported that combustion of biomass materials can also contribute to the PAHs in the atmosphere (Simoneit, 2002;Ge et al., 2012;Young et al., 2016). In this study, PAHs correlated weakly with levoglucosan during the whole sampling period (R^2=0.27). Yet the concentrations of total PAHs in P1 (18.6±11 ng m^{-3}) are nearly 8 times higher than those in P2 (2.3±1.0 ng m^{-3}). These results mean that although the emission of biomass burning is not the most important source for PAHs during the entire period, the intensified regional burning of wheat straw in P1 can also enhance the PAHs concentration in the atmosphere of Gucheng.

As shown in Figure 9, all the primary aerosol markers mentioned above showed lower concentrations in daytime with lowest concentrations at afternoon (12:00-18:00 pm), consisting with the favorable diffusion conditions caused by high temperature and planetary boundary layer (PBL). However, the day-night variation of PAHs, hopanes, and phthalate esters are more obvious than other species, again confirming the lower contribution of biomass burning to these organic compositions.

3.3.5 Secondary organic aerosols (SOA) tracers

Eight compounds were identified as isoprene oxidation products in the $PM_{2.5}$

samples, including two methyltetrahydrofuran diols, three C_5-alkene triols, two 2-methyltetrols, and 2-methylglyceric acid (Table S1). Detailed information about formation and contribution of these compositions were discussed in our previous paper (Li et al., 2018). The concentrations of total detected isoprene-derived products are 112±86 ng m^{-3}, with much higher concentration in P1 (209±105 ng m^{-3}) than in P2 (57±29 ng m^{-3}).

cis-Pinonic acid (PNA), pinic acid (PA), 3-hydroxyglutaric acid (HGA) and 3-methyl-1,2,3-butanetricarboxylic acid (MBTCA) were detected as tracers for α-/β-pinene oxidation in this study, and their concentration are shown in Table S1. The concentration of total detected α-/β-pinene oxidation tracers are 66±31 ng m^{-3}, with MBTCA (31±14 ng m^{-3}) being the major compound during the whole sampling period. PNA and PA are considered as first-generation products of α-/β-pinene oxidation. They can be produced by further oxidation of carbonyl-substituted Criegee intermediates formed by α-pinene ozonolysis (Jenkin et al., 2000;Ma et al., 2008), or by OH oxidation of α-pinene under NO_x free conditions (Eddingsaas et al., 2012;Xuan et al., 2015). The formation of 3-HGA is supposed to be based on a ring opening mechanism and may be related to a heterogeneous reaction of these monoterpenes with irradiation in the presence of NOx (Jaoui et al., 2005;Claeys et al., 2007). As shown in Figure 6b-d, PNA, PA and HGA present similar temporal variations and correlated well with each other (R^2=0.48-0.76, Figure S4). The formation of MBTCA is explained by further photodegradation of *cis*-pinonic acid and pinic acid with OH radical (Müller et al., 2012;Szmigielski et al., 2007). As a

later-generation oxidation products, MBTCA showed an obviously different temporal variation profile than those of PNA and PA, and had no significant increase during P1. In addition, the concertation of PNA, PA and HGA in P1 are 2-8 times higher than those in P2. However, the concentration of MBTCA in the two periods are comparable. These results are consistent with the longer time scales of formation pathway, lower volatility and longer lifetime of MBTCA in the atmosphere compared to the first-generation products of α-/β-pinene oxidation. β-Caryophyllinic acid, formed either by ozonolysis or photo-oxidation of β-caryophyllene (a sesquiterpene) (Jaoui et al., 2007), was also determined in this study, and its concentration ranged from 0.49 to 78 ng m^{-3} (Ave. 17±17 ng m^{-3}). The mean concentration of β-caryophyllinic acid in P1 is 35±21 ng m^{-3}, being 5 times higher than that in P2 (4.1±1.2 ng m^{-3}).

Undoubtedly, the combustion of biomass materials can release a large amount of volatile organic compounds, including isoprene and terpenoids (Andreae and Merlet, 2001). As shown in Figure 5 and 6, the total biogenic SOA tracers, the sum of detected tracers of isoprene, α-/β-pinene, and β-caryophyllene derived SOA, showed a similar temporal variation pattern as levoglucosan with a moderate correlation (R^2=0.56, Figure S5a). Specifically, levoglucosan showed strong linearly correlations with 3-hydroxyglutaric acid (R^2=0.72) (Figure 8c) and β-caryophyllinic acid (R^2=0.80) (Figure 8d), indicating a significant contribution of biomass burning emissions to the formation of SOA derived from mono- and sesqui- terpene oxidation. In our previous paper (Li et al., 2018), we discussed the different diurnal variations of

444 isoprene-derived SOA tracers. In this study, the diurnal variations of other SOA
445 tracers are shown in Figure 10. All the SOA tracers presented weaker day-night
446 variations compared to primary organic aerosol markers, because of the competition
447 between the enhanced daytime formation by photoxidation and the nighttime
448 accumulation associated with a low PBL. Yet, there are some differences between
449 these SOA tracers. For example, PNA and PA presented lowest concentrations in the
450 afternoon (12:00-18:00 pm) due to their relatively high volatilities, which is
451 unfavorable for gas-to-aerosol phase partitioning. However, the later-generation
452 product of PNA and PA, i.e., the less volatile MBTCA, continuously increased during
453 the daytime.

454 Two classes of aromatic SOA markers, phthalic acids and
455 2,3-dihydroxy-4-oxopentanoic acid (DHOPA), were detected in the samples as well.
456 Phthalic acids are believed to be produced by the oxidation of naphthalene and other
457 PAHs (Kawamura et al., 2005;Kawamura and Ikushima, 1993;Kanakidou et al., 2005).
458 The mean concentrations of total phthalic acids in the whole sampling period ranged
459 from 17 to 487 ng m^{-3} with a mean value of 155±94 ng m^{-3}. Their different temporal
460 variation patterns than levoglucosan suggest that biomass burning emission
461 contributes little to phthalic acids formation in the region. The DHOPA was
462 considered to be a tracer compound for toluene-derived SOA (Kleindienst et al., 2004).
463 DHOPA presented a similar temporal variation and moderate correlation to
464 levoglusoan (R^2=0.51, Figure S5b), indicating a certain contribution of biomass
465 burning. Similar to MBTCA, the volatility of DHOPA is quite low, and thus mainly

exists in the particle phase at field temperature (Ding et al., 2017). Thus, DHOPA showed a similar diurnal variation to MBTCA, with higher concentrations during daytime.

3.4 Assessment of source contributions

In order to investigate the differences in organic aerosol sources between the two representative periods, we first classified all the measured organic compounds into seven different sources: (a) "plant emission" represented by higher plant wax n-alkanes, HMW fatty acids and fatty alcohols ($\geqslant C_{20}$); (b) "fossil fuel combustion" mainly represented by fossil fuel derived n-alkanes, hopanes, and PAHs; (c) "biomass burning" represented by levoglucosan and its isomers; (d) "marine/microbial source" represented by LMW fatty acids ($<C_{20}$); (e) "soil/fungal spore/pollen" represented by primary saccharides and sugar alcohols; (f) "plastic emission" represented by phthalate esters; and (g) "secondary oxidation" represented by biogenic SOA tracers, DHOPA, and phthalic acids. The concentrations of individual classes and their contributions to OC content during P1 and P2 are summarized in Figure 11. Plant emission-derived compounds accounted for a larger fraction of $PM_{2.5}$ OC during P1 than during P2 (mean fractions of 28.7 ± 9.3‰ in P1 vs. 16.5 ±7.2‰ in P2). The average faction of biomass burning-derived organics in P1 was also higher in P1 than in P2 (6.0 ± 3.9‰ vs. 4.6 ± 2.1‰), so do organics derived from soil/fungal spore/pollen. However, organic molecules from the other 4 sources all presented a higher contribution to OC in P2 than in P1.

While the relative abundances of organic tracer compounds in $PM_{2.5}$ offer some

Atmos. Chem. Phys. Discuss., https://doi.org/10.5194/acp-2019-75
Manuscript under review for journal Atmos. Chem. Phys.
Discussion started: 25 April 2019

Atmospheric Chemistry and Physics Discussions

488 insights into the relative contributions of different sources to organic aerosols, the
489 estimation is only qualitative because there is a potential overlapping occurrence of
490 many organic species from multiple sources (Simoneit et al., 2004b). In this study we
491 used a tracer-based source apportionment method to access the contributions of
492 certain primary and secondary sources to aerosol OC in the atmosphere of the rural
493 site. As described above, two samples collected at 21st Jun 18:00-24:00 pm were
494 considered to be highly affected by the direct emission from biomass burning nearby
495 the sampling site. Thus, the average OC/levoglucosan ratio in the smoke of biomass
496 burning （$\left(\frac{OC}{Levo}\right)_{BB}$） can be estimated by the followed equation:

497 $$\left(\frac{OC}{Levo}\right)_{BB} = \frac{OC_n - \frac{1}{2}(OC_{before} + OC_{after})}{Levo_n - \frac{1}{2}(Levo_{before} + Levo_{Levo})} \quad (E1)$$

498 Where OC_n and $Levo_n$ are the average concentrations of OC and levoglucosan in
499 the two samples affected by nearby sources. OC_{before} and $Levo_{before}$ are the
500 concentrations of OC and levoglucosan in the sample before this event, whereas
501 OC_{after} and $Levo_{after}$ are the concentrations of OC and levoglucosan in the sample after
502 it. The mean values in the "before" and the "after" samples were subtracted to
503 minimize the influence of local background contribution. The calculated $\left(\frac{OC}{Levo}\right)_{BB}$ in
504 this study is 18.7, which is somewhat higher than the average value of 12.3 measured
505 in Rondônia aerosols (Graham et al., 2002). This difference can be attributed to the
506 differences of biomass fuels in the two regions. For other sources, the measured
507 concentrations of mannitol were used to calculate the contributions of fungal spores to
508 OC (Bauer et al., 2008), and SOA tracers were used to estimate the SOC formed from
509 the oxidation of isoprene, α-/β-pinene, β-caryophyllene, and toluene (Kleindienst et

al., 2007). Also, these tracer-based approaches tend to have large uncertainties, especially for SOC estimation (Li et al., 2013a). However, our results are still meaningful to understand the relative abundances of organic aerosols from these sources in different periods.

As shown in Figure 12, biomass-burning derived OC, ranging from 0.11-27.5 μgC m^{-3}, is the dominant source, which accounts for 1.16-74.8% (ave. 22.6%) of OC in the aerosols of the rural region during the whole sampling period. Fungal-spore derived OC (0.003-5.12 μgC m^{-3}) is a minor source, only accounting for 0.43% (0.003-5.12%) of OC. The contribution of total SOC derived from oxidation of isoprene, α-/β-pinene, β-caryophyllene, and toluene to OC ranged from 5.90-34.1% with an average at 16.7%. Among the four SOC precursors, toluene-derived products accounted for 7.78% (2.06-21.7%) of OC, being the most important SOC contributor. The relative abundances of these sources showed clear temporal variations during the whole sampling period (Figure 12). The contribution of biomass burning derived OC to total OC in P1 (27.6%) was 1.7 times of that in P2 (17.1%) (Figure 13), further indicating the strong regional impact of open-field wheat straw burning on the molecular compositions of organic aerosols in the rural area of NCP. The contribution of SOC from oxidation of the four VOCs increased slightly from P1 (16.3%) to P2 (21.1%). It should be noted that biomass burning can also release a large amount of VOCs, which may produce more secondary organic aerosols during the long-range transport. Thus, the impact of intensified biomass burning in the southern region of NCP on organic aerosols in the Gucheng area is likely even stronger than the

estimation presented above with implications for regional climate.

4. Summary and Conclusion

During the entire sampling period, OC and WSOC showed strong positive correlations with levoglucosan, and the diurnal variation of WSOC/OC was similar to that of levoglucosan/OC, suggesting that summertime organic aerosols in the rural area of NCP are highly affected by direct emission of BB. Higher relative abundances and CPI values of HMW n-alkanes, fatty acids and fatty alcohols in P1 indicated an enhancing effect of open-field biomass burning on molecular composition of organic aerosols. PAHs, hopanes, and phthalate esters presented different temporal and diurnal variations from levoglucosan because of the lower contribution of BB to these organic compositions. The total biogenic SOA tracers showed a similar temporal variation and a moderate correlation with levoglucosan, demonstrating the enhancing effect of BB emission on BSOA formation. Later-generation SOA products, e.g., MBTCA in this study, are unlikely affected directly by BB emission, and thus show little changes in concentrations between the two periods. The source distribution results derived using a tracer-based method demonstrated that the contribution of BB to organic aerosols increased by more than 50% during the period influenced by regional open-field biomass burning (P1) compared to the period when local emissions were more dominant (P2). However, this contribution may even be underestimated since BB can also release a large amount of VOCs enhancing the formation of SOA in the atmosphere. Our results confirmed that intensified field burning of biomass fuels can significantly influence the concentration and composition of aerosols, and thus affect

554 atmospheric chemistry and climate on a regional scale.

555

556 **Author Contributions**

557 G.H. Wang designed the experiment. G.H. Wang, T. Zhu and L.M. Zeng arranged the
558 sample collection. J.J. Li. and G.H. Wang collected the samples. J.J. Li, G.H. Wang, J.
559 Li, C. Wu and W.Q. Jiang analyzed the samples. J.J. Li, and G.H. Wang performed the
560 data interpretation. J.J. Li, G.H. Wang and Q. Zhang wrote the paper.
561
562

563 **Acknowledgements**

564 This work was financially supported by the program from National Nature Science
565 Foundation of China (No. 41773117, 91543116, 41405122). The authors gratefully
566 acknowledge the use of fire spots data products from the Land, Atmosphere Near
567 real-time Capability for EOS (LANCE) system operated by the NASA/GSFC/Earth
568 Science Data and Information System (ESDIS) with funding provided by NASA/HQ
569 (https://firms.modaps.eosdis.nasa.gov/firemap/), and the NOAA Air Resources
570 Laboratory (ARL) for the provision of the HYSPLIT transport and dispersion model
571 and/or READY website (http://www.ready.noaa.gov) used in this publication.
572
573
574

575 **Reference**

576 Aggarwal, S. G., Kawamura, K., Umarji, G. S., Tachibana, E., Patil, R. S., and Gupta, P. K.: Organic
577 and inorganic markers and stable C-, N-isotopic compositions of tropical coastal aerosols from
578 megacity Mumbai: sources of organic aerosols and atmospheric processing, Atmos. Chem. Phys.,
579 13, 4667-4680, 10.5194/acp-13-4667-2013, 2013.
580 Andreae, M. O., and Merlet, P.: Emission of trace gases and aerosols from biomass burning, Global
581 Biogeochemical Cycles, 15, 955-966, 10.1029/2000gb001382, 2001.
582 Andreae, M. O., and Rosenfeld, D.: Aerosol–cloud–precipitation interactions. Part 1. The nature and
583 sources of cloud-active aerosols, Earth-Science Reviews, 89, 13-41,
584 10.1016/j.earscirev.2008.03.001, 2008.
585 Chan, M. N., Choi, M. Y., Ng, N. L., and Chan, C. K.: Hygroscopicity of water-soluble organic
586 compounds in atmospheric aerosols: Amino acids and biomass burning derived organic species,
587 Environ. Sci. Technol., 39, 1555-1562, 10.1021/es049584l, 2005.
588 Claeys, M., Szmigielski, R., Kourtchev, I., Van der Veken, P., Vermeylen, R., Maenhaut, W., Jaoui, M.,
589 Kleindienst, T. E., Lewandowski, M., Offenberg, J. H., and Edney, E. O.: Hydroxydicarboxylic
590 Acids: Markers for Secondary Organic Aerosol from the Photooxidation of α-Pinene, Environ.
591 Sci. Technol., 41, 1628-1634, 10.1021/es0620181, 2007.
592 Dinar, E., Anttila, T., and Rudich, Y.: CCN activity and hygroscopic growth of organic aerosols
593 following reactive uptake of ammonia, Environ. Sci. Technol., 42, 793-799, 10.1021/es071874p,
594 2008.
595 Ding, X., Zhang, Y. Q., He, Q. F., Yu, Q. Q., Wang, J. Q., Shen, R. Q., Song, W., Wang, Y. S., and Wang,

X. M.: Significant Increase of Aromatics-Derived Secondary Organic Aerosol during Fall to Winter in China, Environ. Sci. Technol., 51, 7432-7441, 10.1021/acs.est.6b06408, 2017.

Eddingsaas, N. C., Loza, C. L., Yee, L. D., Chan, M., Schilling, K. A., Chhabra, P. S., Seinfeld, J. H., and Wennberg, P. O.: alpha-pinene photooxidation under controlled chemical conditions - Part 2: SOA yield and composition in low- and high-NOx environments, Atmos. Chem. Phys., 12, 7413-7427, 10.5194/acp-12-7413-2012, 2012.

Engling, G., Lee, J. J., Tsai, Y. W., Lung, S. C. C., Chou, C. C. K., and Chan, C. Y.: Size-Resolved Anhydrosugar Composition in Smoke Aerosol from Controlled Field Burning of Rice Straw, Aerosol Science and Technology, 43, 662-672, 10.1080/02786820902825113, 2009.

Fabbri, D., Marynowski, L., Fabianska, M. J., Zaton, M., and Simoneit, B. R. T.: Levoglucosan and other cellulose markers in pyrolysates of miocene lignites: Geochemical and environmental implications, Environ. Sci. Technol., 42, 2957-2963, 10.1021/es7021472, 2008.

Fabbri, D., Torri, C., Simoneit, B. R. T., Marynowski, L., Rushdi, A. I., and Fabiańska, M. J.: Levoglucosan and other cellulose and lignin markers in emissions from burning of Miocene lignites, Atmos. Environ., 43, 2286-2295, 2009.

Fu, P. Q., Kawamura, K., Pavuluri, C. M., Swaminathan, T., and Chen, J.: Molecular characterization of urban organic aerosol in tropical India: contributions of primary emissions and secondary photooxidation, Atmos. Chem. Phys., 10, 2663-2689, 2010.

Fu, P. Q., Kawamura, K., Chen, J., Li, J., Sun, Y. L., Liu, Y., Tachibana, E., Aggarwal, S. G., Okuzawa, K., Tanimoto, H., Kanaya, Y., and Wang, Z. F.: Diurnal variations of organic molecular tracers and stable carbon isotopic composition in atmospheric aerosols over Mt. Tai in the North China Plain: an influence of biomass burning, Atmos. Chem. Phys., 12, 8359-8375, 10.5194/acp-12-8359-2012, 2012.

Ge, X., Setyan, A., Sun, Y., and Zhang, Q.: Primary and secondary organic aerosols in Fresno, California during wintertime: Results from high resolution aerosol mass spectrometry, Journal of Geophysical Research: Atmospheres, 117, n/a-n/a, 10.1029/2012jd018026, 2012.

Graham, B., Mayol-Bracero, O. L., Guyon, P., Roberts, G. C., Decesari, S., Facchini, M. C., Artaxo, P., Maenhaut, W., Koll, P., and Andreae, M. O.: Water-soluble organic compounds in biomass burning aerosols over Amazonia - 1. Characterization by NMR and GC-MS, J. Geophys. Res.-Atmos., 107, DOI:804710.801029/802001jd000336, 2002.

Guo, S., Hu, M., Zamora, M. L., Peng, J., Shang, D., Zheng, J., Du, Z., Wu, Z., Shao, M., Zeng, L., Molina, M. J., and Zhang, R.: Elucidating severe urban haze formation in China, Proceedings of the National Academy of Sciences of the United States of America, 111, 17373-17378, 10.1073/pnas.1419604111, 2014.

Halek, F., Nabi, G., and Kavousi, A.: Polycyclic aromatic hydrocarbons study and toxic equivalency factor (TEFs) in Tehran, IRAN, Environmental Monitoring and Assessment, 143, 303-311, 10.1007/s10661-007-9983-9, 2008.

Hallquist, M., Wenger, J. C., Baltensperger, U., Rudich, Y., Simpson, D., Claeys, M., Dommen, J., Donahue, N. M., George, C., Goldstein, A. H., Hamilton, J. F., Herrmann, H., Hoffmann, T., Iinuma, Y., Jang, M., Jenkin, M. E., Jimenez, J. L., Kiendler-Scharr, A., Maenhaut, W., McFiggans, G., Mentel, T. F., Monod, A., Prevot, A. S. H., Seinfeld, J. H., Surratt, J. D., Szmigielski, R., and Wildt, J.: The formation, properties and impact of secondary organic aerosol: current and emerging issues, Atmos. Chem. Phys., 9, 5155-5236, 2009.

Huang, R. J., Zhang, Y. L., Bozzetti, C., Ho, K. F., Cao, J. J., Han, Y. M., Daellenbach, K. R., Slowik, J.

640 G., Platt, S. M., Canonaco, F., Zotter, P., Wolf, R., Pieber, S. M., Bruns, E. A., Crippa, M., Ciarelli,
641 G., Piazzalunga, A., Schwikowski, M., Abbaszade, G., Schnelle-Kreis, J., Zimmermann, R., An, Z.
642 S., Szidat, S., Baltensperger, U., El Haddad, I., and Prevot, A. S. H.: High secondary aerosol
643 contribution to particulate pollution during haze events in China, Nature, 514, 218-222,
644 10.1038/nature13774, 2014.
645 Jaoui, M., Kleindienst, T. E., Lewandowski, M., Offenberg, J. H., and Edney, E. O.: Identification and
646 quantification of aerosol polar oxygenated compounds bearing carboxylic or hydroxyl groups. 2.
647 Organic tracer compounds from monoterpenes, Environ. Sci. Technol., 39, 5661-5673,
648 10.1021/es048111b, 2005.
649 Jaoui, M., Lewandowski, M., Kleindienst, T. E., Offenberg, J. H., and Edney, E. O.: β-caryophyllinic
650 acid: An atmospheric tracer for β-caryophyllene secondary organic aerosol, Geophysical Research
651 Letters, 34, doi:10.1029/2006GL028827, 2007.
652 Jenkin, M. E., Shallcross, D. E., and Harvey, J. N.: Development and application of a possible
653 mechanism for the generation of cis -pinic acid from the ozonolysis of α - and β -pinene, Atmos.
654 Environ., 34, 2837-2850, 2000.
655 Jimenez, J. L., Canagaratna, M. R., Donahue, N. M., Prevot, A. S. H., Zhang, Q., ., Kroll, J. H., Decarlo,
656 P. F., Allan, J. D., Coe, H., ., and Ng, N. L.: Evolution of organic aerosols in the atmosphere,
657 Science, 326, 1525-1529, 2009.
658 Kanakidou, M., Seinfeld, J. H., Pandis, S. N., Barnes, I., Dentener, F. J., Facchini, M. C., Van Dingenen,
659 R., Ervens, B., Nenes, A., Nielsen, C. J., Swietlicki, E., Putaud, J. P., Balkanski, Y., Fuzzi, S.,
660 Horth, J., Moortgat, G. K., Winterhalter, R., Myhre, C. E. L., Tsigaridis, K., Vignati, E., Stephanou,
661 E. G., and Wilson, J.: Organic aerosol and global climate modelling: a review, Atmos. Chem.
662 Phys., 5, 1053-1123, 2005.
663 Kawamura, K., and Ikushima, K.: Seasonal changes in the distribution of dicarboxylic acids in the
664 urban atmosphere, Environ. Sci. Technol., 27, 2227-2235, 1993.
665 Kawamura, K., Kosaka, M., and Sempere, R.: Distributions and seasonal changes in hydrocarbons in
666 urban aerosols and rain waters, Chikyu Kagaku (Geochemistry), 29, 1-15 (In Japanese), 1995.
667 Kawamura, K., Ishimura, Y., and Yamazaki, K.: Four years' observations of terrestrial lipid class
668 compounds in marine aerosols from the western North Pacific, Global Biogeochemical Cycles, 17,
669 10.1029/2001gb001810, 2003.
670 Kawamura, K., Imai, Y., and Barrie, L. A.: Photochemical production and loss of organic acids in high
671 Arctic aerosols during long-range transport and polar sunrise ozone depletion events, Atmos.
672 Environ., 39, 599-614, 10.1016/j.atmosenv.2004.10.020, 2005.
673 Kleindienst, T. E., Conver, T. S., McIver, C. D., and Edney, E. O.: Determination of secondary organic
674 aerosol products from the photooxidation of toluene and their implications in ambient PM2.5, J.
675 Atmos. Chem., 47, 79-100, 2004.
676 Kleindienst, T. E., Jaoui, M., Lewandowski, M., Offenberg, J. H., Lewis, C. W., Bhave, P. V., and
677 Edney, E. O.: Estimates of the contributions of biogenic and anthropogenic hydrocarbons to
678 secondary organic aerosol at a southeastern US location, Atmos. Environ., 41, 8288-8300,
679 10.1016/j.atmosenv.2007.06.045, 2007.
680 Kondo, Y., Miyazaki, Y., Takegawa, N., Miyakawa, T., Weber, R. J., Jimenez, J. L., Zhang, Q., and
681 Worsnop, D. R.: Oxygenated and water-soluble organic aerosols in Tokyo, Journal of Geophysical
682 Research, 112, 10.1029/2006jd007056, 2007.
683 Lelieveld, J., Evans, J. S., Fnais, M., Giannadaki, D., and Pozzer, A.: The contribution of outdoor air

pollution sources to premature mortality on a global scale, Nature, 525, 367-371, 10.1038/nature15371, 2015.

Li, J. J., Wang, G. H., Cao, J. J., Wang, X. M., and Zhang, R. J.: Observation of biogenic secondary organic aerosols in the atmosphere of a mountain site in central China: temperature and relative humidity effects, Atmos. Chem. Phys., 13, 11535-11549, 10.5194/acp-13-11535-2013, 2013a.

Li, J. J., Wang, G. H., Wang, X. M., Cao, J. J., Sun, T., Cheng, C. L., Meng, J. J., Hu, T. F., and Liu, S. X.: Abundance, composition and source of atmospheric PM 2.5 at a remote site in the Tibetan Plateau, China, Tellus B, 65, doi:10.3402/tellusb.v3465i3400.20281, 2013b.

Li, J. J., Wang, G. H., Wu, C., Cao, C., Ren, Y. Q., Wang, J. Y., Li, J., Cao, J. J., Zeng, L. M., and Zhu, T.: Characterization of isoprene-derived secondary organic aerosols at a rural site in North China Plain with implications for anthropogenic pollution effects, Scientific reports, 8, DOI: 10.1038/s41598-41017-18983-41597, 10.1038/s41598-017-18983-7, 2018.

Li, W. J., Shao, L. Y., and Buseck, P. R.: Haze types in Beijing and the influence of agricultural biomass burning, Atmos. Chem. Phys., 10, 8119-8130, 10.5194/acp-10-8119-2010, 2010.

Li, Y. J., Sun, Y., Zhang, Q., Li, X., Li, M., Zhou, Z., and Chan, C. K.: Real-time chemical characterization of atmospheric particulate matter in China: A review, Atmos. Environ., 158, 270-304, 10.1016/j.atmosenv.2017.02.027, 2017.

Li, Z. Q., Xia, X. G., Cribb, M., Mi, W., Holben, B., Wang, P. C., Chen, H. B., Tsay, S. C., Eck, T. F., Zhao, F. S., Dutton, E. G., and Dickerson, R. R.: Aerosol optical properties and their radiative effects in northern China, J. Geophys. Res.-Atmos., 112, 10.1029/2006jd007382, 2007.

Müller, L., Reinnig, M. C., Naumann, K. H., Saathoff, H., Mentel, T. F., Donahue, N. M., and Hoffmann, T.: Formation of 3-methyl-1,2,3-butanetricarboxylic acid via gas phase oxidation of pinonic acid – a mass spectrometric study of SOA aging, Atmos. Chem. Phys., 12, 1483-1496, 10.5194/acp-12-1483-2012, 2012.

Ma, Y., Russell, A. T., and Marston, G.: Mechanisms for the formation of secondary organic aerosol components from the gas-phase ozonolysis of alpha-pinene, Physical Chemistry Chemical Physics, 10, 4294-4312, 10.1039/b803283a, 2008.

Oros, D. R., and Simoneit, B. R. T.: Identification and emission rates of molecular tracers in coal smoke particulate matter, Fuel, 79, 515-536, http://dx.doi.org/10.1016/S0016-2361(99)00153-2, 2000.

Quan, J. N., Gao, Y., Zhang, Q., Tie, X. X., Cao, J. J., Han, S. Q., Meng, J. W., Chen, P. F., and Zhao, D. L.: Evolution of planetary boundary layer under different weather conditions, and its impact on aerosol concentrations, Particuology, 11, 34-40, 10.1016/j.partic.2012.04.005, 2013.

Rogge, W. F., Hildemann, L. M., Mazurek, M. A., Cass, G. R., and Simoneit, B. R. T.: Sources of Fine Organic Aerosols .4. Particulate Abrasion Products from Leaf Surfaces of Urban Plants, Environ. Sci. Technol., 27, 2700-2711, 1993a.

Rogge, W. F., Hildemann, L. M., Mazurek, M. A., Cass, G. R., and Simoneit, B. R. T.: Sources of Fine Organic Aerosols. 2. Noncatalyst and Catalyst-equipped Automobile and Heavy-duty Diesel Trucks, Environ. Sci. Technol., 27, 636-651, 1993b.

Shen, Z., Zhang, Q., Cao, J., Zhang, L., Lei, Y., Huang, Y., Huang, R. J., Gao, J., Zhao, Z., Zhu, C., Yin, X., Zheng, C., Xu, H., and Liu, S.: Optical properties and possible sources of brown carbon in PM 2.5 over Xi'an, China, Atmos. Environ., 150, 322-330, 10.1016/j.atmosenv.2016.11.024, 2017.

Simoneit, B. R. T., Schauer, J. J., Nolte, C. G., Oros, D. R., Elias, V. O., Fraser, M. P., Rogge, W. F., and Cass, G. R.: Levoglucosan, a tracer for cellulose in biomass burning and atmospheric particles,

Atmos. Environ., 33, 173-182, 1999.

Simoneit, B. R. T.: Biomass burning - A review of organic tracers for smoke from incomplete combustion, Applied Geochemistry, 17, 129-162, 2002.

Simoneit, B. R. T., Elias, V. O., Kobayashi, M., Kawamura, K., Rushdi, A. I., Medeiros, P. M., Rogge, W. F., and Didyk, B. M.: Sugars - Dominant water-soluble organic compounds in soils and characterization as tracers in atmospheric particulate matter, Environ. Sci. Technol., 38, 5939-5949, 10.1021/es0403099, 2004a.

Simoneit, B. R. T., Kobayashi, M., Mochida, M., Kawamura, K., Lee, M., Lim, H. J., Turpin, B. J., and Komazaki, Y.: Composition and major sources of organic compounds of aerosol particulate matter sampled during the ACE-Asia campaign, J. Geophys. Res.-Atmos., 109, D19S10, 10.1029/2004jd004598, 2004b.

Sultan, C., Balaguer, P., Terouanne, B., Georget, V., Paris, F., Jeandel, C., Lumbroso, S., and Nicolas, J. C.: Environmental xenoestrogens, antiandrogens and disorders of male sexual differentiation, Molecular and Cellular Endocrinology, 178, 99-105, 10.1016/s0303-7207(01)00430-0, 2001.

Sun, Y. L., Jiang, Q., Wang, Z. F., Fu, P. Q., Li, J., Yang, T., and Yin, Y.: Investigation of the sources and evolution processes of severe haze pollution in Beijing in January 2013, J. Geophys. Res.-Atmos., 119, 4380-4398, 10.1002/2014jd021641, 2014.

Sun, Y. L., Jiang, Q., Xu, Y. S., Ma, Y., Zhang, Y. J., Liu, X. G., Li, W. J., Wang, F., Li, J., Wang, P. C., and Li, Z. Q.: Aerosol characterization over the North China Plain: Haze life cycle and biomass burning impacts in summer, J. Geophys. Res.-Atmos., 121, 2508-2521, 10.1002/2015jd024261, 2016.

Szmigielski, R., Surratt, J. D., Gomez-Gonzalez, Y., Van der Veken, P., Kourtchev, I., Vermeylen, R., Blockhuys, F., Jaoui, M., Kleindienst, T. E., Lewandowski, M., Offenberg, J. H., Edney, E. O., Seinfeld, J. H., Maenhaut, W., and Claeys, M.: 3-methyl-1,2,3-butanetricarboxylic acid: An atmospheric tracer for terpene secondary organic aerosol, Geophysical Research Letters, 34, L24811, 10.1029/2007gl031338, 2007.

Tie, X. X., Huang, R. J., Dai, W. T., Cao, J. J., Long, X., Su, X. L., Zhao, S. Y., Wang, Q. Y., and Li, G. H.: Effect of heavy haze and aerosol pollution on rice and wheat productions in China, Scientific reports, 6, 10.1038/srep29612, 2016.

van Donkelaar, A., Martin, R. V., Brauer, M., Kahn, R., Levy, R., Verduzco, C., and Villeneuve, P. J.: Global Estimates of Ambient Fine Particulate Matter Concentrations from Satellite-Based Aerosol Optical Depth: Development and Application, Environmental Health Perspectives, 118, 847-855, 10.1289/ehp.0901623, 2010.

Venkataraman, C., Habib, G., Eiguren-Fernandez, A., Miguel, A. H., and Friedlander, S. K.: Residential biofuels in south Asia: Carbonaceous aerosol emissions and climate impacts, Science, 307, 1454-1456, 10.1126/science.1104359, 2005.

Wang, G. H., and Kawamura, K.: Molecular characteristics of urban organic aerosols from Nanjing: A case study of a mega-city in China, Environ. Sci. Technol., 39, 7430-7438, 10.1021/es051055+, 2005.

Wang, G. H., Kawamura, K., Lee, S., Ho, K. F., and Cao, J. J.: Molecular, seasonal, and spatial distributions of organic aerosols from fourteen Chinese cities, Environ. Sci. Technol., 40, 4619-4625, 10.1021/es060291x, 2006a.

Wang, G. H., Kawamura, K., Watanabe, T., Lee, S. C., Ho, K. F., and Cao, J. J.: High loadings and source strengths of organic aerosols in China, Geophysical Research Letters, 33,

L2280110.1029/2006gl027624, 2006b.

Wang, G. H., Kawamura, K., Umemoto, N., Xie, M. J., Hu, S. Y., and Wang, Z. F.: Water-soluble organic compounds in PM2.5 and size-segregated aerosols over Mount Tai in North China Plain, J. Geophys. Res.-Atmos., 114, D1920810.1029/2008jd011390, 2009a.

Wang, G. H., Kawamura, K., Xie, M. J., Hu, S. Y., Cao, J. J., An, Z. S., Waston, J. G., and Chow, J. C.: Organic Molecular Compositions and Size Distributions of Chinese Summer and Autumn Aerosols from Nanjing: Characteristic Haze Event Caused by Wheat Straw Burning, Environ. Sci. Technol., 43, 6493-6499, 10.1021/es803086g, 2009b.

Wang, G. H., Chen, C. L., Li, J. J., Zhou, B. H., Xie, M. J., Hu, S. Y., Kawamura, K., and Chen, Y.: Molecular composition and size distribution of sugars, sugar-alcohols and carboxylic acids in airborne particles during a severe urban haze event caused by wheat straw burning, Atmos. Environ., 45, 2473-2479, 10.1016/j.atmosenv.2011.02.045, 2011.

Wang, G. H., Zhang, R. Y., Gomez, M. E., Yang, L. X., Zamora, M. L., Hu, M., Lin, Y., Peng, J. F., Guo, S., Meng, J. J., Li, J. J., Cheng, C. L., Hu, T. F., Ren, Y. Q., Wang, Y. S., Gao, J., Cao, J. J., An, Z. S., Zhou, W. J., Li, G. H., Wang, J. Y., Tian, P. F., Marrero-Ortiz, W., Secrest, J., Du, Z. F., Zheng, J., Shang, D. J., Zeng, L. M., Shao, M., Wang, W. G., Huang, Y., Wang, Y., Zhu, Y. J., Li, Y. X., Hu, J. X., Pan, B., Cai, L., Cheng, Y. T., Ji, Y. M., Zhang, F., Rosenfeld, D., Liss, P. S., Duce, R. A., Kolb, C. E., and Molina, M. J.: Persistent sulfate formation from London Fog to Chinese haze, Proceedings of the National Academy of Sciences of the United States of America, 113, 13630-13635, 10.1073/pnas.1616540113, 2016.

Xuan, Z., Renee C, M., Dan D, H., Nathan F, D., Bernard, A., Richard C, F., and John H, S.: Formation and evolution of molecular products in α-pinene secondary organic aerosol, Proceedings of the National Academy of Sciences of the United States of America, 112, 14168-14173, 2015.

Young, D. E., Kim, H., Parworth, C., Zhou, S., Zhang, X., Cappa, C. D., Seco, R., Kim, S., and Zhang, Q.: Influences of emission sources and meteorology on aerosol chemistry in a polluted urban environment: results from DISCOVER-AQ California, Atmos. Chem. Phys., 16, 5427-5451, 10.5194/acp-16-5427-2016, 2016.

Zhang, J. K., Cheng, M. T., Ji, D. S., Liu, Z. R., Hu, B., Sun, Y., and Wang, Y. S.: Characterization of submicron particles during biomass burning and coal combustion periods in Beijing, China, The Science of the total environment, 562, 812-821, 10.1016/j.scitotenv.2016.04.015, 2016.

Zhang, Q., Jimenez, J. L., Canagaratna, M. R., Allan, J. D., Coe, H., Ulbrich, I., Alfarra, M. R., Takami, A., Middlebrook, A. M., and Sun, Y. L.: Ubiquity and dominance of oxygenated species in organic aerosols in anthropogenically-influenced Northern Hemisphere midlatitudes, Geophysical Research Letters, 34, L13801, 2007.

Zhang, Q., Streets, D. G., Carmichael, G. R., He, K. B., Huo, H., Kannari, A., Klimont, Z., Park, I. S., Reddy, S., Fu, J. S., Chen, D., Duan, L., Lei, Y., Wang, L. T., and Yao, Z. L.: Asian emissions in 2006 for the NASA INTEX-B mission, Atmos. Chem. Phys., 9, 5131-5153, 10.5194/acp-9-5131-2009, 2009.

Zhu, Y., Yang, L., Chen, J., Wang, X., Xue, L., Sui, X., Wen, L., Xu, C., Yao, L., Zhang, J., Shao, M., Lu, S., and Wang, W.: Characteristics of ambient volatile organic compounds and the influence of biomass burning at a rural site in Northern China during summer 2013, Atmos. Environ., 124, 156-165, 10.1016/j.atmosenv.2015.08.097, 2016.

Atmos. Chem. Phys. Discuss., https://doi.org/10.5194/acp-2019-75
Manuscript under review for journal Atmos. Chem. Phys.
Discussion started: 25 April 2019

Atmospheric Chemistry and Physics Discussions

816 Table 1 Concentrations of carbonaceous components in the time-resolved (3-h) $PM_{2.5}$ samples in
817 the rural site of NCP during the whole sampling period, Period 1 (P1) and Period 2 (P2).

Component	Whole period (N=117)			Period 1 (N=28)			Period 2 (N=13)		
	Range	Mean	SD	Range	Mean	SD	Range	Mean	SD
$PM_{2.5}$ (μg m^{-3})	21~395	159	89	133~347	231	59	21~62	43	14
OC (μg m^{-3})	1.7~45.7	17.3	11.1	13.8~44.4	29.4	7.8	3.6~8.8	5.5	1.7
EC (μg m^{-3})	0.2~22.3	6.5	4.9	5.3~22.3	12.1	4.0	0.9~2.6	1.5	0.5
WSOC (μg m^{-3})	0.7~33.0	11.5	8.2	5.3~33.0	19.1	8.3	1.2~4.2	2.6	0.8
WIOC (μg m^{-3})	0.3~28.1	6.4	5.1	4.5~28.1	10.3	4.4	1.2~5.5	3.0	1.3
OC/EC	1.2~7.6	3.0	0.9	1.9~3.2	2.5	0.4	2.5~5.7	3.8	1.0
WSOC/OC	0.07~0.95	0.63	0.18	0.30~0.85	0.62	0.16	0.18~0.67	0.48	0.12
WIOC/OC	0.05~0.93	0.37	0.18	0.15~0.70	0.38	0.16	0.33~0.82	0.52	0.12

818
819
820

Atmos. Chem. Phys. Discuss., https://doi.org/10.5194/acp-2019-75
Manuscript under review for journal Atmos. Chem. Phys.
Discussion started: 25 April 2019

Atmospheric Chemistry and Physics Discussions

821 Table 2 Average concentrations of the organic compound classes (ng m^{-3}) in the time-resolved (3-h)
822 $PM_{2.5}$ samples in the rural site of NCP during the whole study period, Period 1 (P1) and Period 2
823 (P2).

Compounds	Whole period (N=117)			Period 1 (N=28)			Period 2 (N=13)		
	Range	Mean	SD	Range	Mean	SD	Range	Mean	SD
n-Alkanes	9.97~722.2	206.9	149.3	94.7~722.3	343.7	134.1	25.1~103.2	54.3	22.4
CPI (C_{18}-C_{36})[a]	1.08~8.62	2.47	1.12	1.38~4.67	2.85	0.87	1.08~3.5	1.64	0.59
Fatty acids	64.6~1777	514.4	384.3	206.7~1528	900.3	358.3	81.4~234.4	145.3	47.7
CPI ($C_{21:0}$-$C_{30:0}$)[b]	2.26~9.15	4.24	1.14	3.49~6.11	4.21	0.64	2.26~8.57	3.50	1.64
Fatty alcohols	3.18~975.9	192.6	187.4	62.4~638.2	322.0	150.7	16.6~100.2	33.9	22.6
Sugar compounds	15.9~2228	432.8	428.9	151.9~1727	718.0	403.1	39.7~241.3	93.2	52.9
galactosan (G)	1.03~97.78	18.5	20.6	2.16~97.8	29.5	27.9	1.45~13.3	4.61	3.13
mannosan (M)	0.69~54.82	9.78	10.4	1.61~54.8	15.0	13.3	0.96~6.63	2.83	1.43
levoglucosan (L)	5.56~1447	240.1	287.8	29.3~1428	404.0	344.0	11.2~123	47.8	26.2
L/M ratio	4.03~71.8	22.8	8.85	13.9~71.8	29.7	12.2	11.3~23.1	18.0	4.28
L/(G+M) ratio	1.38~19.3	8.05	2.59	5.3~19.3	10.1	3.41	4.58~10.2	6.77	1.97
PAHs	1.11~48.5	12.0	11.0	4.21~37.7	18.6	11.0	1.25~5.01	2.33	0.98
Hopanes	0.66~10.81	3.46	2.38	0.86~9.97	4.40	2.48	1.14~2.28	1.81	0.31
Phthalate esters	17.7~219.9	84.9	41.3	68.8~183.1	111.5	32.7	31.5~100.8	51.1	18.1
Phthalic acids	17.1~487.2	154.5	93.9	91.3~388.6	211.0	87.1	17.1~81	46.3	17.1
Isoprene SOA tracers	11.1~404.1	111.9	85.8	48.3~404.1	208.5	104.9	34.8~127.5	57.0	29.4
Monoterpene SOA tracers	11.1~166.2	66.1	31.2	37.3~166.2	85.3	34.9	26.7~64.5	44.6	12.6
β-Caryophyllinic acid[c]	0.49~77.7	17.4	17.1	4.6~77.8	34.7	20.8	2.44~6.28	4.08	1.21
DHOPA[d]	1.59~35.3	9.36	7.15	4.06~35.3	15.6	9.80	2.7~6.99	4.16	1.42
Total measured organics	176.9~6249	1806	1308	843.3~5499	2973	1219	334.2~913.7	537.9	151.1
Total organics_C/OC[e] (%)	3.19~16.0	6.99	1.97	3.43~8.86	6.43	1.36	3.77~8.61	6.41	1.27

824 [a] CPI (C_{18}-C_{36}): carbon preference index for *n*-alkanes, (C_{19}+C_{21}+C_{23}+C_{25}+C_{27}+C_{29}+C_{31}+C_{33}+C_{35})/
825 (C_{18}+C_{20}+C_{22}+C_{24}+C_{26}+C_{28}+C_{30}+C_{32}+C_{34}).
826 [b] CPI ($C_{21:0}$-$C_{30:0}$): carbon preference index for fatty acids, ($C_{22:0}$+$C_{24:0}$+$C_{26:0}$+$C_{28:0}$+$C_{30:0}$)/ ($C_{21:0}$+$C_{23:0}$+$C_{25:0}$+$C_{27:0}$+$C_{29:0}$).
827 [c] *β*-Caryophyllinic acid: a tracer of *β*-caryophyllene-derived SOA.
828 [d] DHOPA: 2,3-dihydroxy-4-oxopentanoic acid, a tracer of toluene-derived SOA.
829 [e] All the quantified organic compounds were converted to their carbon contents to calculate the OC ratios.

Atmos. Chem. Phys. Discuss., https://doi.org/10.5194/acp-2019-75
Manuscript under review for journal Atmos. Chem. Phys.
Discussion started: 25 April 2019

Atmospheric Chemistry and Physics Discussions

Figure Captions

Figure 1. Backward trajectories of air masses (a,c) (provided by NOAA HYSPLIT modeling system, http://ready.arl.noaa.gov/HYSPLIT.php), and fire spots (b,d) (provided by Fire Information for Resource Management System, FIRMS, https://firms.modaps.eosdis.nasa.gov/firemap/), during Period 1 (P1) (Jun 13th 21:00-16th 15:00, 2013) and Period 2 (P2) (Jun 22nd 12:00-24th 06:00, 2013). Sampling site represented as purple star.

Figure 2. Temporal variations of $PM_{2.5}$, OC, EC, and WSOC during the whole sampling period. Shadows denote the two representative periods.

Figure 3. Linear correlations of OC with WSOC (a), levoglucosan with OC and WSOC(b).

Figure 4. Diurnal variation of OC/EC (a), WSOC/OC and levoglucosan/OC (b).

Figure 5. Temporal variations of ten organic compound classes detected in the summertime $PM_{2.5}$ samples at the rural site of NCP.

Figure 6. Temporal variations of organic tracers for biomass burning (a), and secondary products derived from *α*-/*β*-pinene (b-d), *β*-caryophyllene (e), and toluene (f).

Figure 7. Molecular distributions of *n*-alkanes (a and d), fatty acids (b and e), and fatty alcohols (c and f) in the $PM_{2.5}$ of the rural area.

Figure 8. Linear correlations of fatty acids (a), fatty alcohols (b), 3-hydroxyglutaric acid (c), and β-caryophyllinic acid (d) with levoglucosan.

Figure 9. Diurnal variation of the detected organic compound classes.

Figure 10. Diurnal variation of the SOA tracers derived from oxidation of *α*-/*β*-pinene (a-d), *β*-caryophyllene (e), and toluene (f).

Figure 11. A comparison of the average contributions of different sources-derived organics (converted to carbon content) to OC during P1 and P2.

Figure 12. Contributions (above) of primary organic carbon from biomass burning (OC_{bb}) and fungal spores (OC_{fp}), and secondary organic carbon from isoprene (SOC_i), *α*-/*β*-pinene (SOC_p), *β*-caryophyllene (SOC_p), and toluene (SOC_t) to OC in the time-resolved (3 h) rural aerosols, and their relative abundances (down). All the contributions were estimated by tracer-based method.

Figure 13. Average contributions of direct emissions from biomass burning (BB) and fungal spores (OC_{fp}), secondary oxidation from isoprene (SOC_i), *α*-/*β*-pinene (SOC_p),*β*-caryophyllene (SOC_p), and toluene (SOC_t) to OC in P1 and P2. All the contributions were estimated by tracer-based method.

Atmos. Chem. Phys. Discuss., https://doi.org/10.5194/acp-2019-75
Manuscript under review for journal Atmos. Chem. Phys.
Discussion started: 25 April 2019

Atmospheric Chemistry and Physics Discussions

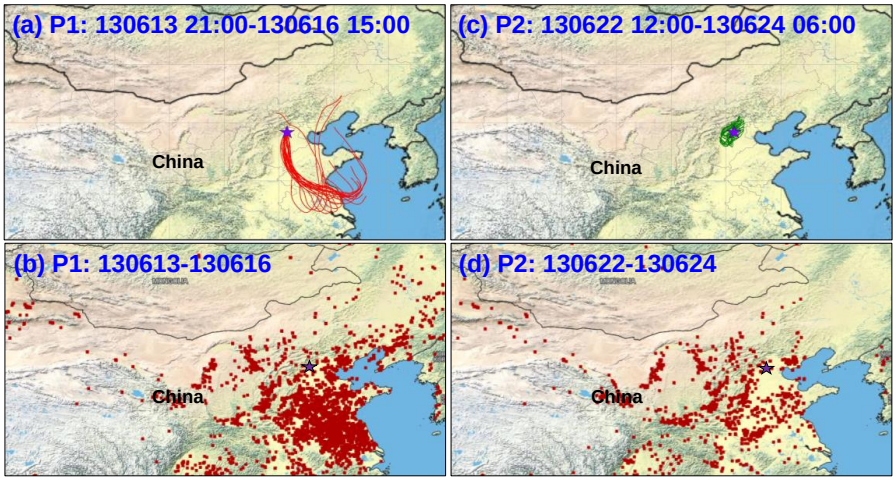

Figure 1. Backward trajectories of air masses (a,c) (provided by NOAA HYSPLIT modeling system, http://ready.arl.noaa.gov/HYSPLIT.php), and fire spots (b,d) (provided by Fire Information for Resource Management System, FIRMS, https://firms.modaps.eosdis.nasa.gov/firemap/), during Period 1 (P1) (Jun 13th 21:00-16th 15:00, 2013) and Period 2 (P2) (Jun 22nd 12:00-24th 06:00, 2013). Sampling site represented as purple star.

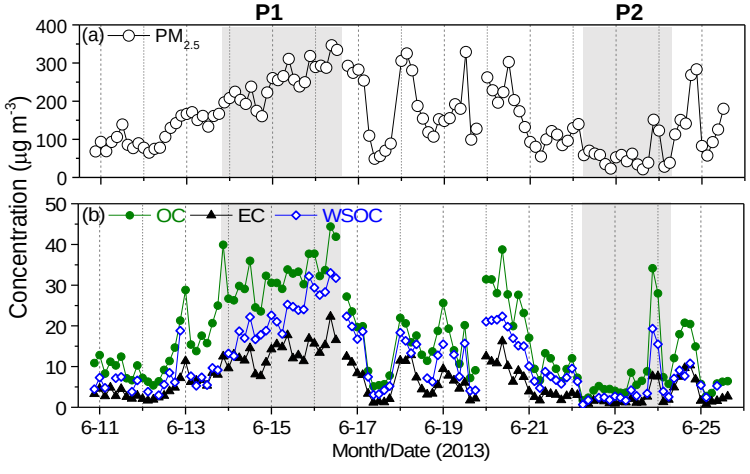

Figure 2. Temporal variations of $PM_{2.5}$, OC, EC, and WSOC during the whole sampling period. Shadows denote the two representative periods.

Atmos. Chem. Phys. Discuss., https://doi.org/10.5194/acp-2019-75
Manuscript under review for journal Atmos. Chem. Phys.
Discussion started: 25 April 2019

Atmospheric Chemistry and Physics Discussions

882

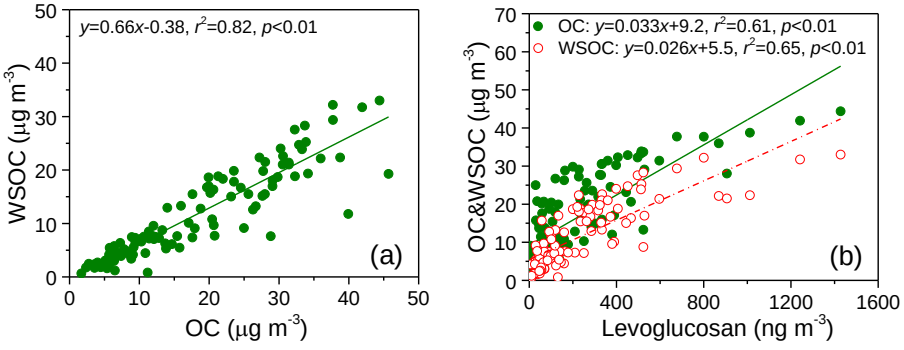

883

884 Figure 3. Linear correlations of OC with WSOC (a), levoglucosan with OC and WSOC(b).

885

886

887

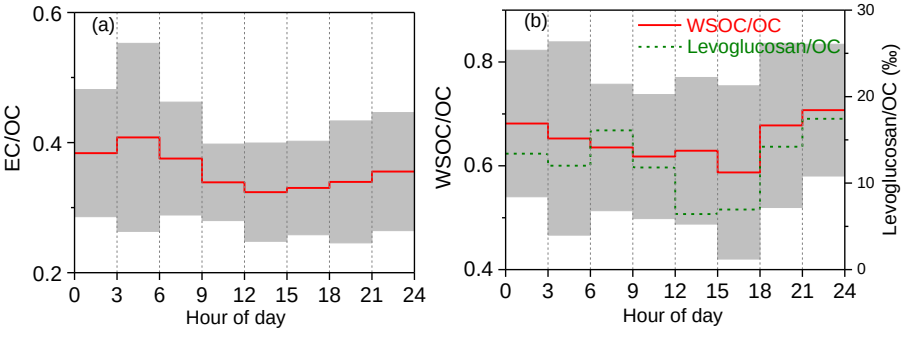

888

889 Figure 4. Diurnal variation of OC/EC (a), WSOC/OC and levoglucosan/OC (b).

890

Atmos. Chem. Phys. Discuss., https://doi.org/10.5194/acp-2019-75
Manuscript under review for journal Atmos. Chem. Phys.
Discussion started: 25 April 2019

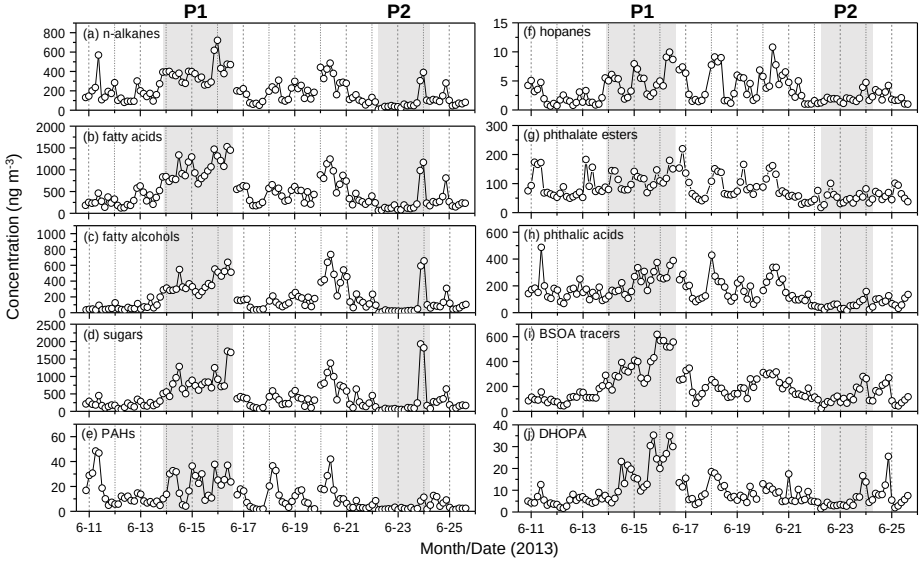

Figure 5. Temporal variations of ten organic compound classes detected in the summertime $PM_{2.5}$ samples at the rural site of NCP.

Atmos. Chem. Phys. Discuss., https://doi.org/10.5194/acp-2019-75
Manuscript under review for journal Atmos. Chem. Phys.
Discussion started: 25 April 2019

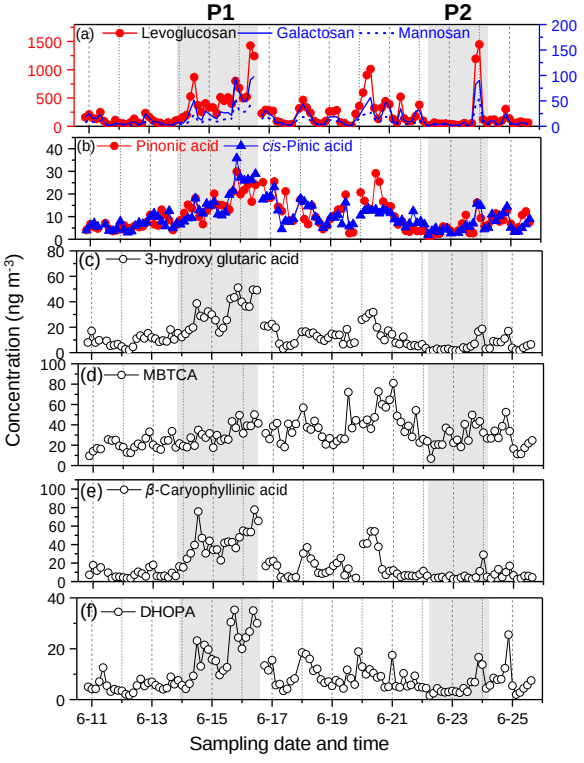

Figure 6. Temporal variations of organic tracers for biomass burning (a), and secondary products derived from *α*-/*β*-pinene (b-d), *β*-caryophyllene (e), and toluene (f).

Atmos. Chem. Phys. Discuss., https://doi.org/10.5194/acp-2019-75
Manuscript under review for journal Atmos. Chem. Phys.
Discussion started: 25 April 2019

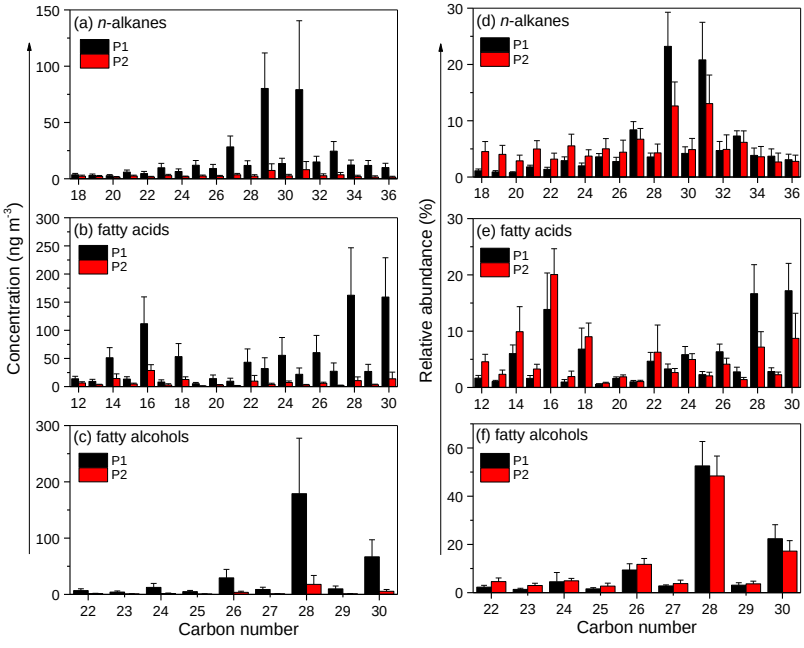

Figure 7. Molecular distributions of *n*-alkanes (a and d), fatty acids (b and e), and fatty alcohols (c and f) in the $PM_{2.5}$ of the rural area.

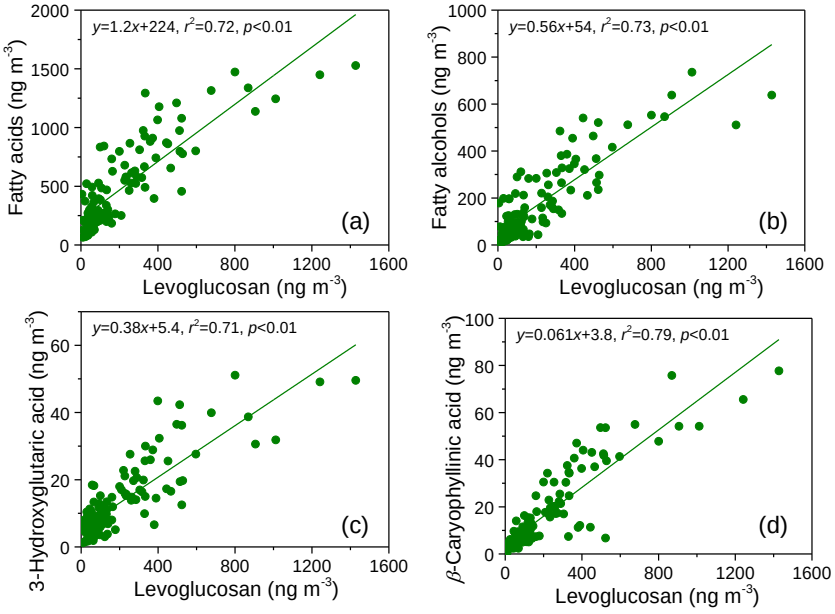

Figure 8. Linear correlations of fatty acids (a), fatty alcohols (b), 3-hydroxyglutaric acid (c), and β-caryophyllinic acid (d) with levoglucosan.

Atmos. Chem. Phys. Discuss., https://doi.org/10.5194/acp-2019-75
Manuscript under review for journal Atmos. Chem. Phys.
Discussion started: 25 April 2019

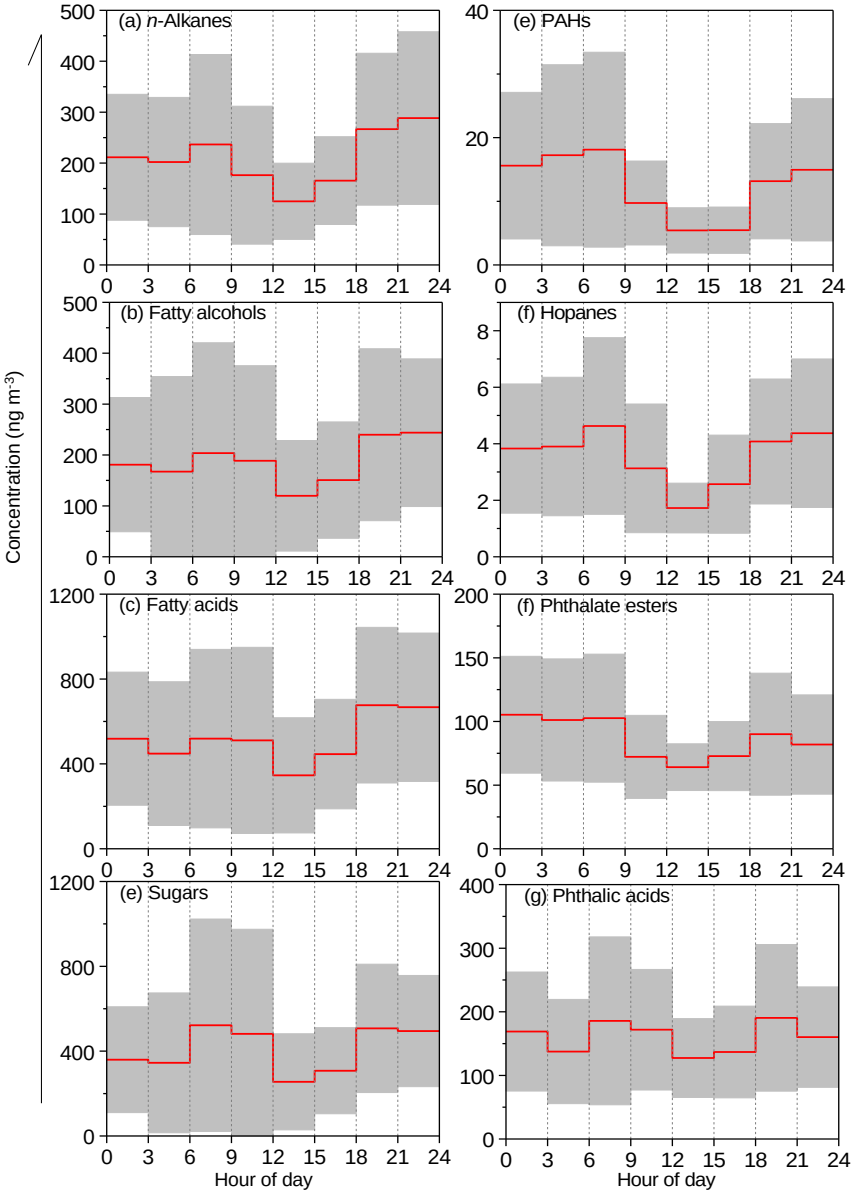

Figure 9. Diurnal variation of the detected organic compound classes.

Atmos. Chem. Phys. Discuss., https://doi.org/10.5194/acp-2019-75
Manuscript under review for journal Atmos. Chem. Phys.
Discussion started: 25 April 2019

Atmospheric Chemistry and Physics Discussions

914

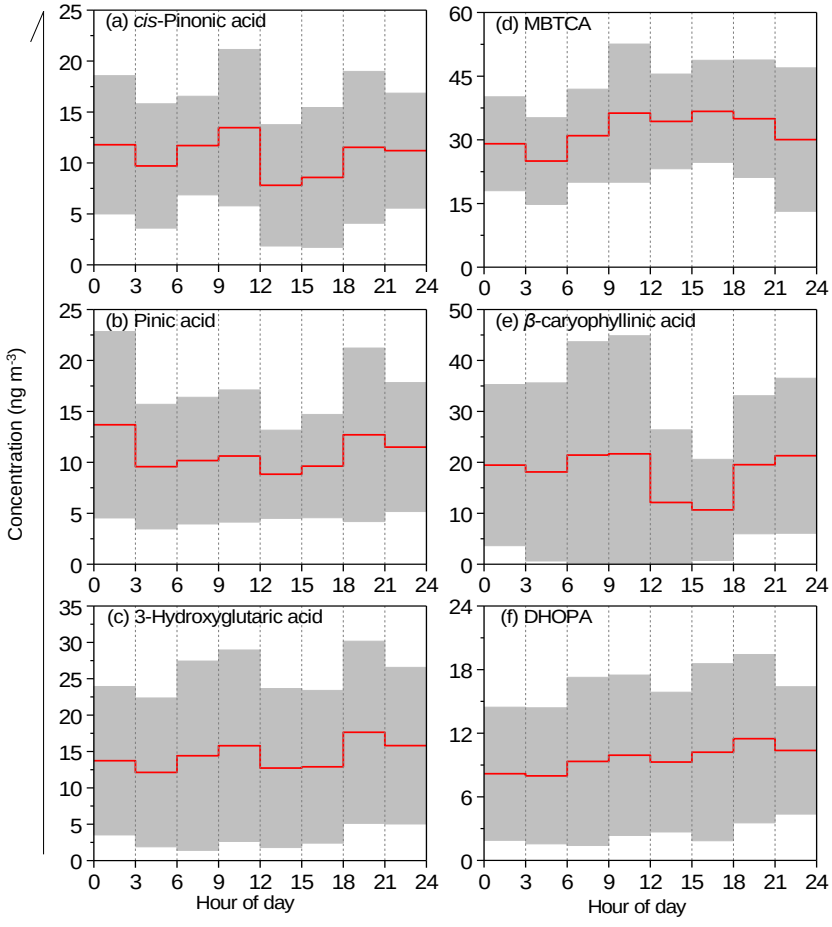

915

916 Figure 10. Diurnal variation of the SOA tracers derived from oxidation of *α*-/*β*-pinene (a-d),
917 *β*-caryophyllene (e), and toluene (f).

918

919

Atmos. Chem. Phys. Discuss., https://doi.org/10.5194/acp-2019-75
Manuscript under review for journal Atmos. Chem. Phys.
Discussion started: 25 April 2019

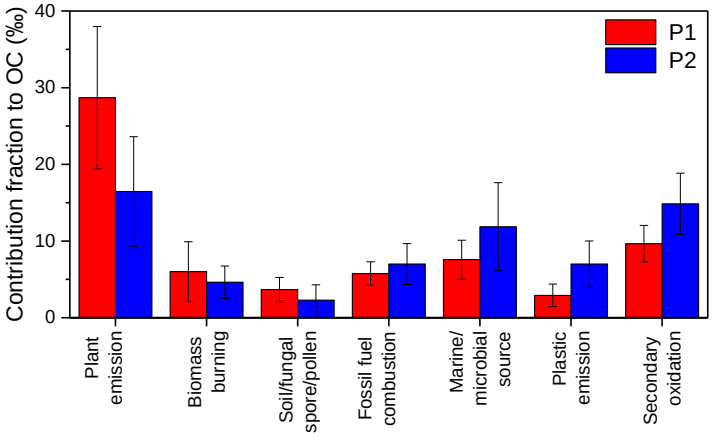

Figure 11 A comparison of the average contributions of different sources-derived organics (converted to carbon content) to OC during P1 and P2.

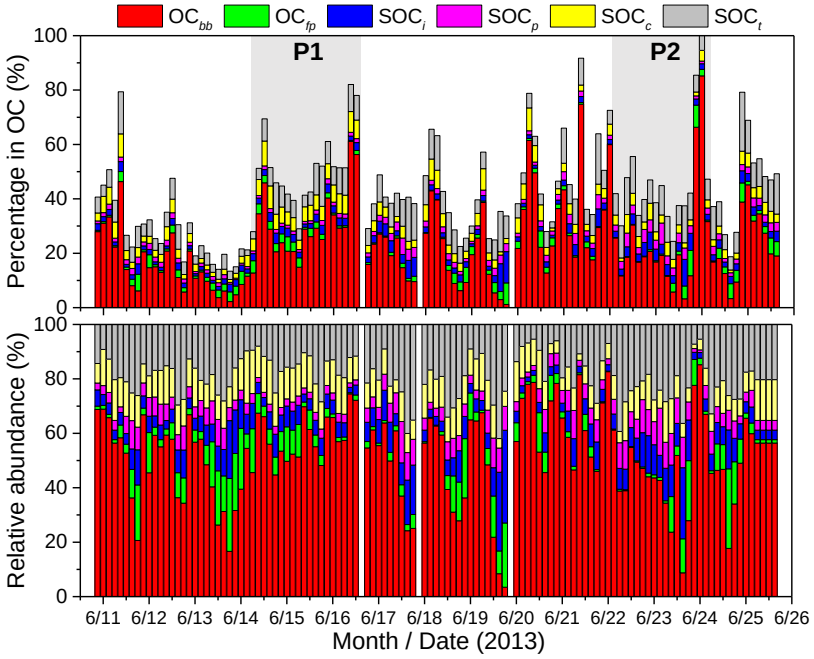

Figure 12. Contributions (above) of primary organic carbon from biomass burning (OC_{bb}) and fungal spores (OC_{fp}), and secondary organic carbon from isoprene (SOC_i), *α*-/*β*-pinene (SOC_p), *β*-caryophyllene (SOC_p), and toluene (SOC_t) to OC in the time-resolved (3 h) rural aerosols, and their relative abundances (down). All the contributions were estimated by tracer-based method.

Atmos. Chem. Phys. Discuss., https://doi.org/10.5194/acp-2019-75
Manuscript under review for journal Atmos. Chem. Phys.
Discussion started: 25 April 2019

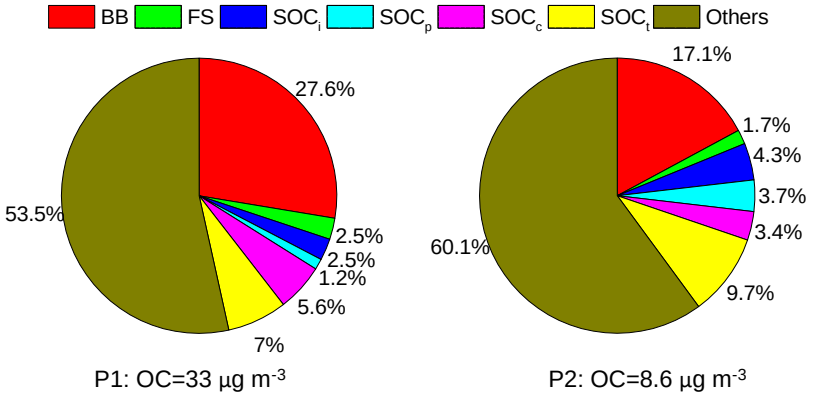

Figure 13. Average contributions of direct emissions from biomass burning (BB) and fungal spores (OC_{fp}), secondary oxidation from isoprene (SOC_i), α-/β-pinene (SOC_p),β-caryophyllene (SOC_p), and toluene (SOC_t) to OC in P1 and P2. All the contributions were estimated by tracer-based method.